Directing neuronal outgrowth and network formation of rat cortical neurons by cyclic substrate stretch

Jella-Andrea Abraham[1], Christina Linnartz[1], Georg Dreissen[1], Ronald Springer[1], Stefan Blaschke[2,3] Maria A. Rueger[2,3], Gereon R. Fink[2,3], Bernd Hoffmann[1*], Rudolf Merkel[1]

[1] Research Centre Jülich, Institute of Complex Systems (ICS-7): Biomechanics, Jülich, Germany

[2] Department of Neurology, University Hospital of Cologne, Cologne, Germany

[3] Research Centre Jülich, Institute of Neuroscience and Medicine (INM-3): Cognitive Neuroscience, Jülich, Germany

*To whom correspondence should be addressed

Dr. Bernd Hoffmann: Institute of Complex Systems, ICS-7
Forschungszentrum Jülich
52425 Jülich, Germany
Tel.: ++49 (0)2461 61 6734
Email: b.hoffmann@fz-juelich.de

Keywords: cyclic stretch, cell mechanics, neuronal network formation, Tubulin, MAP2

Abstract

Neuronal mechanobiology plays a vital function in brain development and homeostasis with an essential role in neuronal maturation, pathfinding, and differentiation but is also crucial for understanding brain pathology. In this study, we constructed an *in vitro* system to assess neuronal responses to cyclic strain as a mechanical signal. The selected strain amplitudes mimicked physiological as well as pathological conditions. By subjecting embryonic neuronal cells to cyclic uniaxial strain we could steer the direction of neuronal outgrowth perpendicular to strain direction for all applied amplitudes. A long-term analysis proved maintained growth direction. Moreover, stretched neurons showed an enhanced length, growth, and formation of nascent side branches with most elevated growth rates subsequent to physiological straining. Application of cyclic strain to already formed neurites identified retraction bulbs with destabilized microtubule structures as spontaneous responses. Importantly, neurons were able to adapt to the mechanical signals without induction of cell death and showed a triggered growth behavior when compared to unstretched neurons. The data suggest that cyclic strain plays a critical role in neuronal development.

Introduction

The human brain consists of billions of neurons that form over a trillion synaptic connections. Recent studies on neural and cerebral biomechanics emphasize a central role of mechanical forces in neuronal development and the formation of synapses.[1-2] However, the need for a better understanding of the healthy development of the brain and the impact of disease, e.g., a stroke or traumatic brain injury, how this complex system is regulated, and how numerous connections with specific targets are formed, is contrasted by the dearth of data regarding the mechanobiology of neurons. Physiologically, cortical neurons are well embedded in a soft environment of extracellular matrix proteins and surrounded by soft supporting glial cells.[3] Comparing the neuronal cytoskeleton to cells with a clear association to mechanical strain, e.g., cells of the vasculature, it is therefore widely assumed that cortical neurons are less equipped to bear mechanical loads (see, e.g., Reference [4]).

In neurons, one vital cytoskeletal component are microtubules that span through the neuronal extensions. Since microtubules are relatively stiff,[5] and hence poorly equipped to bear mechanical loads,[6] it has been suggested that neuronal extensions are solely ripped apart when exposed to strain.[7] Microtubules interact with adapter proteins, for example the microtubule associated protein 2 (MAP2) [8] that defines the stabilization of the microtubule cytoskeleton.[9] It controls its rigidity,[9] crosslinks actin filaments to microtubules,[9] and protects the cytoskeletal structure from severing enzymes.[10] Through dimerization, microtubule associated proteins (MAPs) can form bridges to a nearby microtubule and thereby promote the formation of microtubule bundles.[11] It has been suggested that mechanical loads result in a failure to build such cross-links.[12] Accordingly, to date, most studies of neuronal biomechanics focused on mechanical force induced diseases rather than considering mechanical cues as a developmental trigger.[2] In contrast, recent studies outlined that sensing mechanical cues may be fundamental for neuronal cell development.[13-16] Indeed, mechanical stretch alone induced neuronal differentiation and axonal outgrowth in human neuroblastoma cells and identified enhanced growth rates for

static stretch conditions with possibly ion channels as mechanosensitive elements.[14-17]

Although most mechanobiological studies in neuroscience focus on cellular responses to static strain,[15-19] neuronal cells are exposed to cyclic strain throughout their lifetime. Even mild heart beat leads to brain tissue deformation by 5% [20] and may even be significantly higher during embryogenesis and brain development.[21] Furthermore, everyday cranial accelerations stretch and compress brain tissue. Likewise, body motion and brain perfusion result in cyclic tissue deformation in the 2% range measured at the resolution of magnetic resonance imaging.[22] At the much higher resolution of intracranial microscopy, frequent diameter changes of brain blood vessels of up to 30% on a time scale of some few seconds were observed.[23-24] All these effects sum up to significant cyclic straining of human brain tissue in daily life. Furthermore, without an exact knowledge of the thresholds for inducing pathology, repetitive events such as vibration,[20, 25] shaking,[25-26] shear deformation,[20, 26] and frequent pressure changes [20] may all play a critical role in inducing mechanical injury.

We here present an in vitro model for accurate application and control of physiological as well as pathological strain parameters which allows the systematic exploration of the neuronal cells' response to mechanical stimuli of physiological relevance. We observed that neuronal cells are surprisingly resilient to mechanical loads and that mechanical stress does not automatically lead to apoptosis. Instead, cyclic strain regulated outgrowth and growth direction and even enhanced neuronal growth and side branch formation over a broad amplitude range.

Experimental section

Fabrication of elastomeric culture chambers

The generation of flexible cell culture substrates was performed as described before.[27] As a result stretching chambers made of cross-linked polydimethylsiloxane (PDMS) (Sylgard 184, Dow Corning, Wiesbaden, Germany) with a Young's modulus of 50 kPa and a Poisson ratio of 0.5 were used. Base polymer was mixed in a 1:40 ratio with its cross-linking agent. We avoided procedures that might alter physicochemical properties of the elastomer surface like plasma treatment or UV exposure. Therefore transient effects like hydrophobic recovery [28] were avoided and chambers exhibited shelf lives of some months. The elastomer chambers were mounted in a homemade stretcher device and pre-stretched by 1.5 mm to avoid sacking. Before cell seeding, elastomer chambers were coated with 0.01% poly-L-lysine (150,000-300,000 Mol wt) at room temperature overnight and washed twice with distilled water

Primary cortical neurons isolation

Embryonic rat cortical neurons were obtained from pregnant rats (Wistar, Charles River, Sulzfeld) at 18-19 days of gestation (Animal testing license: 84-02.04.2015.A173, LANUV NRW, Germany). Before decapitation, rats were anesthetized with CO_2. The embryos were surgically removed from the adult rat and kept in ice cold Hanks' Balanced Salt Solution (Sigma, Taufkirchen, Germany). Cortices were isolated from embryonic brains and further trypsinized in 0.05% trypsin-EDTA (ethylenediaminetetraacetic acid) solution (Thermo Fisher Scientific, Massachusetts, USA) for 15 min at 37 °C. The tissue was transferred to pre-warmed neurobasal media (Thermo Fisher Scientific, Massachusetts, USA), supplemented with GlutaMAX (Thermo Fisher Scientific, Massachusetts, USA), B-27 (Thermo Fisher Scientific, Massachusetts, USA) and Gentamicin (Sigma, Taufkirchen, Germany). Cortices were washed three times to remove remaining trypsin solution. Subsequently, cortical cells were dissociated by trituration. A number of 250 cells

per mm^2 was seeded in 500 µL neurobasal media. Half of the medium within the stretching chamber was changed every two days.

Cyclic stretch experiments on outgrowing neurons

Cyclic stretch experiments were performed with cortical cells after 24 h of cultivation to allow the cells to recover and to adhere after isolation. Upon stretching, medium was changed every 12 h. All stretch experiments were performed under sterile conditions in a humidified environment containing 5% CO_2. For the stretch experiments a uniaxial strain with various strain amplitudes (7%, 15% or 28%) and a repeat frequency of 300 mHz (trapezoidal approximation of sine wave) was applied. After cyclic stretch, the stretcher was stopped at pre-stretch position and the chamber holders were removed from the stretch apparatus. Cells were fixed with pre-warmed 3.7% solution of formaldehyde in osmolarity-adjusted cytoskeletal buffer (CB) for 15 min. The fixation reaction was stopped by adding pre-warmed 30 mM glycine in CB for 10 min at room temperature and washed again with 30 mM glycine CB buffer.

Live/dead staining and flow cytometry

To analyze vitality after strain, cells were observed before and after stretch with differential interference contrast (DIC) live cell microscopy and an upright microscope Imager M2 (Carl Zeiss, Germany) and a 20x 0.5 NA water N Achroplan objective. Additionally, cells were also stained with 2 µM ethidium homodimer and analyzed by flow cytometry (Guava EasyCyte, Merck Millipore, Darmstadt, Germany). After trypsinizing the cells from the culture chambers, neurons were fixed with 10% of solution A from FIX and PERM Cell Fixation and Cell Permeabilization Kit (Thermo Fisher Scientific, Massachusetts, USA) in phosphate buffered saline (PBS) for 5 min and resuspended in PBS to analyze the number of dead cells. As positive control for induced cell death camptothecin [29] in a concentration of 5 µM was added 24 h before cell fixation.

Immunofluorescent labeling of MAP2 and tubulin

Immunofluorescent labeling of MAP2 and tubulin was performed in the PDMS culture chambers as described before.[30] As primary antibodies, anti-MAP2 (1:500 dilution, Millipore, AB5622) and anti-tubulin YL1/2 (1:200 dilution, Millipore, MAB1864) were used. Alexa Fluor 647 (chicken anti-rat) and Alexa Fluor 488 (chicken anti-rabbit) labeled secondary antibodies were used in 1:200 and 1:500 dilution, respectively. After immunofluorescent staining, cells were embedded in mounting media containing fluoromount (Sigma, Taufkirchen, Germany) and 15 mM DABCO (1,4-diazabicyclo[2.2.2]octane), and overlaid with a cover slip. The chamber walls were removed and the observation was performed upside down through the coverslip using a Plan-Neofluar 40x Ph3 (NA 1.3) oil objective (Carl Zeiss, Germany) by confocal microscopy (LSM710, Carl Zeiss, Germany, pixel size: 0.09 or smaller) and appropriate filter settings.

Live cell imaging stretch experiments

Live cell stretch experiments were performed with an upright microscope (Imager M2, Carl Zeiss, Germany) equipped with a 10x 0.3 NA air Plan NeoFluar objective or a 40x 0.1 NA water immersion N-Aprochromat DIC VIS-IR objective (both Carl Zeiss, Germany). Neurons were cultivated for 6 days and subjected to substrate strain of 7%, 15%, and 28%, respectively. As internal control live cell microscopy was also performed 30 min prior and after the stretch period. Images were taken every 5 minutes in pre-stretch position. The live cell dye Tubulin Tracker™ Green (Thermo Fisher Scientific, Massachusetts, USA) was utilized to stain the microtubule cytoskeleton. To this end, neurons were incubated with 100 nM dye for 30 min. After three washing steps cells were used for live cell stretch experiments. All images were concatenated and analyzed using ImageJ (NIH).[31]

Quantification of branching

Immunofluorescence micrographs were analyzed by an in-house developed program (Matlab R2017a). This program enabled automated measurements of

neurite lengths, branch orientations, numbers of branching (nodal) and end points, as well as orientation and intensity of individual branches (see also Supplementary Figure 1). The algorithm was adapted from Li *et al.* [32]

In detail, images were scaled to a common pixel size of 0.09 µm and smoothed with a narrow Gaussian kernel (0.5 pixel). Masks were created for each neuron and both channels (MAP2, tubulin). A first mask contained cell body and neurites. This full mask was determined by segmentation with the mean intensity of the image as intensity threshold. In order to reduce artifacts, morphological processes were used. Morphological opening (disk-shaped structure, radius 2 pixels) removed small-scale structures. In addition, objects smaller than 500 pixels were discarded. Subsequently, morphological closing (disk, 10 pixels radius) was performed to fill small holes in the foreground. The result was used as full mask. As cell bodies exhibited higher intensities than neurites, masks containing cell bodies alone could be determined again by intensity thresholding. This time the threshold value was the mean image intensity plus one standard deviation of the latter. Morphological opening (disk, radius 20 pixels) was performed to remove all remaining thin protrusions. Moreover, all objects smaller than 1000 pixels were removed. To finally create the mask for neurites alone the cell body mask was subtracted from the initial mask. All further analyses were based on the dendrite mask (MAP2 or tubulin) that followed dendrites visibly closer.

This dendrite mask was skeletonized. Using the respective Matlab commands, nodal and endpoints of the branched dendrite network were determined. For statistical analysis each line connecting two nodal points or one nodal point to an end point was considered as branch. Length of branches was simply taken from the length of the skeletonized path. Orientations of branches were calculated as the direction of the longer half axis of ellipses fitted to them. For the construction of angular distributions branches were weighted by their length. Furthermore, MAP2 and tubulin grey values within a branch were determined from the dendrite mask. Finally, distributions of MAP2 and tubulin intensities depending on the orientation towards the stretch direction were constructed.

Statistics

One-sided Kolmogorov-Smirnov (KS) was used to analyze if data were normally distributed. Distributions were not normal. Therefore, comparisons between two different data sets were performed with two-sided KS and Mann-Whitney U test. Only if both tests revealed significance, levels are indicated. The highest p-value between both tests was indicated with * for p-values <0.05, ** for <0.01 and *** for <0.001. The number of independent experiments is indicated in the figure legends.

Results and Discussion

Neuronal cells survive high strain amplitudes and adapt to cyclic varying strain

To investigate how neuronal cells respond to mechanical cues during their development, isolated cortical rat neurons were cyclically stretched during outgrowth 24 h after adhesion with mild amplitudes of 7% and 15% and also with a harsh amplitude of 28%. Cortical neurons survived all examined amplitudes without any morphological changes suggesting apoptosis (Figure 1A). Rather, neurons grew in an undisturbed fashion and continued to extend their neuronal processes despite the constant cyclic strain. Further analysis by flow cytometry confirmed no enhanced cell death of neuronal cells after 24 h of cyclic strain, even at highest strain amplitudes (Figure 1C). Cortical neurons also survived very long periods of cyclic strain with a basically unaffected ability to develop extensions and to form neuronal networks, as shown exemplary for neurons stretched with 15% strain for 6 days (Figure 1B).

These results indicate that cortical neurons adapt to mechanical strain, and as part of their response may even extend their neurites. As both amplitude and frequency are important modulators of cellular responses to cyclic strain,[33] we decided to focus on various amplitudes and to maintain frequency constant throughout all experiments. Since varying frequencies mainly affect response velocity,[33] amplitude-dependent conformational changes of mechanosensitive proteins have been described as the primary signal.[34-35] However, since strain-induced unfolding-refolding kinetics are also strongly affected by frequency changes, causing a reciprocal relationship between strain-specific frequency and amplitude changes,[36-38] additional experiments using various frequencies might help to further elucidate neuronal mechanosensitivity.

Cyclic stretch directs neuronal branch formation

Long-term cyclic strain experiments (Figure 1B) indicate that neuronal cells undergoing significant levels of cyclic strain not only survive but also display directed outgrowth of neurites with a preferred branch direction away from main strain direction. In order to analyze this hypothesis in more detail, we performed a quantitative analysis of main branch orientation after 24 h of cyclic stretch by digital image processing as detailed in the section on quantification of branching in Materials and Methods and Supplementary Figure 1. While lack of strain resulted in a neuronal outgrowth in all directions (with an average orientation of 45°) (Figure 2), already low strain amplitudes of 7% steered neuronal outgrowth away from the applied strain direction (59°). This effect became more pronounced with increasing amplitudes to ultimately reach average main branch orientations of 64° for 15% strain amplitudes, and of 70° for 28% strain amplitudes.

Interestingly, angular distributions of strain-induced directed growth of cortical neurons very much resemble cyclic strain-induced actin reorientation.[27, 35] Previous studies showed that depending on cell type and stretch condition, cells reorient. This happens above a certain threshold in stretch amplitude and frequency and serves to maintain mechanical homeostasis. Intriguingly both stress and strain have been described as control signal for this process.[39-42, 35] For identical stretching chambers as used here the zero strain direction was already determined with an angle of 69°.[35] As average branch orientations are close to this value, neuronal outgrowth appears to take place in directions of minimal strain rather than in direction of minimal stress (90°). This minimizes the mechanical load on cytoskeletal structures. At this point we can only speculate if neuronal outgrowth is regulated by similar mechanosensitive mechanisms as described for actin reorientation [36] and if actin itself plays a vital role in this process. However, the

possibility that the highly conserved cytoskeletal reorientation mechanism might also influence directed long-term growth of neurons is intriguing.

Stretched neurons increase branch formation

To verify if neuronal outgrowth and early steps of neuronal network formation are comparable for strain-induced directed neuronal growth and unstretched cells, we quantified the side branch formation as well as the overall length of all extensions formed (Figure 3). For control cells, side branches were formed almost perpendicular to the main neuronal extensions with a median of 23 branches per cell (average 27.3; 95% confidence interval CI_{95} 1.4). Similar results were also found for stretched cells regarding perpendicular outgrowth direction. However, the number of side branches significantly increased for stretched cells with highest numbers for just slightly strained cells (median 30 branches per cell at 7%; average 33.4, CI_{95} 1.2) (Figure 3B). Slightly lower but still clearly elevated numbers of side branches compared to control cells were also formed for cells strained by 15% (median of 28 branches per cell; average 30.9, CI_{95} 1.3) and 28% (median 27; average 30.6, CI_{95} 1.7). Similar results were identified for overall neuronal growth behavior. Here, control cells were able to form extensions with a median sum length of 99 µm 48 h after seeding (average 114 µm, CI_{95} 6 µm). Upon stretch application for the last 24 h, this sum length significantly increased for all stretch amplitudes tested (median values of 130 µm, 119 µm, and 119 µm for 7%, 15%, and 28%, respectively; mean values 145 µm, 134 µm, and 132 µm; CI_{95} 6 µm, 5 µm, 6 µm, and 7 µm, in the same order) (Figure 3C).

In summary these results proved an enhanced growth and branching of neuronal cells upon cyclic stretching. Most noteworthy, the strongest effect was shown for the mild, most physiological strain amplitude of 7%. This argues for potentially optimal cyclic strain conditions during embryogenesis to support best neuronal outgrowth and network formation. However, since all stretch amplitudes induced enhanced growth and branch formation while a directed cell growth in the zero strain direction occurred in parallel, it remains to be elucidated if real straining or some kind of a more general, mechanically induced homeostasis perturbation is primarily

responsible for this effect. Interestingly, also static stretch conditions have been shown to enhance neuronal growth.[15] There it was suggested that the necessity for maintaining axonal integrity would lead to continuous incorporation of cytoskeletal proteins, resulting in strain-induced lengthening. Furthermore, mechanical tension along the axon has been described to be an effective stimulus for neuronal extension and growth.[15, 17] Here, cyclic straining might effectively enhance mechanical tension along the axon even for neurons with directed outgrowth, resulting in an enhanced incorporation of material into the axon.[17] Interestingly, although directed outgrowth occurred in zero strain direction, even at very high amplitudes side branches were stably formed away from the main extensions and therefore in direction of stretch. Detailed analyses of branch formation revealed that structures largely depend on actin polymerization at early stages and that microtubule formation within these branches takes place at later time points.[43-47] Although our stainings for MAP2 and tubulin argue for already formed microtubule networks within side branches, it might be possible that differences in cytoskeletal structures and binding partners between main extensions and side branches might be responsible for the differential mechanosensitive responses of these structures. Going along with this hypothesis are data on neurons mutated for adenomatous polyposis coli (APC) protein.[48] Upon binding, this protein supports microtubule stability while deletion increases neuronal branch formation. Many further examples for the role of cytoskeletal proteins in neuronal branching have been described.[45, 49] These findings also indicate that cyclic stretch might locally destabilize microtubules and thereby might trigger the formation of side branches.

Spontaneous response of neuronal cells to cyclic strain

Since cortical neurons adapted well to ongoing cyclic strain during outgrowth and network formation, we additionally investigated the immediate neuronal response to cyclic strain when applied to already established neuronal networks. Based on live cell microscopy on extensions that grew before stretch, straining induced an immediate growth cone retraction (Figure 4A). Although most often detected for

extensions that grew in strain direction, a retraction was also detectable for neurites with diagonal or perpendicular orientation relative to stretch. In all cases retraction went along with formation of large retraction bulbs behind the retracted growth cone (see also Supplementary movies 1). Higher amplitudes visibly enhanced the magnitude of retraction and the occurrence of multiple retraction bulbs. With ongoing cyclic straining, extensions paused with low intracellular dynamics in their retracted state. Interestingly, after a time period of approximately 30 min of cyclic straining, extensions regained their ability to grow although straining was still in place (see Supplementary Movie 1). Furthermore, this immediate growth response was not characterized by a change in growth direction but followed largely the growth track of the extension before retraction. With ending of straining, growth of extensions remained intact with velocities even higher than before stretch application (mean velocity rates before (0.33 μm/min, s.d. 0.14 μm/min, n=10), during strain (0.65 μm/min, s.d. 0.40 μm/min, n=20) and after stretch (0.86 μm/min, 0.34 μm/min, n=20). To further investigate the nature of formed retraction bulbs we stained microtubule filaments with low concentrations of the live cell dye Tubulin Tracker Green to prevent dye induced dynamics interference. We could show that immediately upon strain induced appearance, bulbs were filled with high amounts of partially curled microtubules (Figure 4B). In contrast, neuronal extensions in front of formed bulbs were free of microtubules.

These data indicate that strain rapidly and heavily affects the neuronal microtubule network. This effect is well understandable because it was reported that low stresses in the 0.4 to 0.5 N/m^2 range are sufficient to strain and rupture microtubules.[6] Also microtubule dynamic instability is well described [50-51] leading to depolymerization of anchored microtubules as a short-term response to strain.[52] Interestingly, retraction is only temporary and extensions regain their ability to grow even with ongoing straining. Here, further experiments are warranted to clarify whether this ability is primarily due to microtubule cytoskeletal remodeling or dependent on actin or neurofilaments. Growth even in direction of strain and different growth velocities before and after stretch might support the possibility of a mainly actin driven process as also known for early steps in side branch

formation.[43-47] How long this process is active and at what time point growth reorientation takes place also needs to be explored in the future.

Tubulin and MAP2 intensities depend on neurite orientation relative to strain

Our data strongly argue for spontaneous cytoskeletal adaptations in response to strain. To analyze this hypothesis also for cells that were stretched for long periods with correspondingly well oriented extensions, we performed MAP2 and tubulin intensity measurements in an angle dependent manner. In control cells MAP2 and tubulin intensities were identical for all extension segments independent of their orientation (Figure 5). Upon strain application, similar results were found for a mild 7% amplitude with almost identical protein intensities independent of neurite fragment orientation for MAP2, and just slightly increased tubulin contents in extensions oriented in perpendicular direction relative to stretch (p-value = 0.05 for MAP2 intensities of branches with an angle of 0°-20° versus 70°-90°; p-value = 0.02 for tubulin). Interestingly, with increasing strain amplitude, the homogeneous and angle independent distribution of tubulin as well as MAP2 changed dramatically. Here, neurite segments with localization in strain direction were characterized by still unaffected protein levels, compared to control, while both protein amounts were significantly enhanced in segments with main angles heading in perpendicular directions. With an almost doubled protein level for 28% amplitude experiments, this effect was even more pronounced for tubulin (p-value < 0.001 for MAP2 and tubulin intensities of branches with an angle of 0°-20° versus 70°-90°). Mean intensities additionally argued for an overall enhanced protein concentration of MAP2 and tubulin after 24 h of stretch compared to control cells.

The data described for tubulin and MAP2 levels on long-term stretched neuronal systems are in good agreement with the identified immediate responses. They indicate significant remodeling of the microtubule cytoskeleton on various timescales and argue for the ability to adapt the microtubule filament system that is

characterized by low rupture forces[6] to allow microtubule formation also in direction of stretch with time. We can only speculate if this ability is due to specific binding partners with an either stiffening or softening effect on microtubules.[47] Also enhanced crosslinking of shortened microtubule might be possible. However, here an attachment of additional proteins would also be necessary and might go along with self-repair mechanisms as also identified for microtubules in response to mechanical stress.[53] Similarly, the clearly increased tubulin and MAP concentrations in reoriented neurites were unexpected. Although directed growth goes along with very low strain levels, a reinforcement of microtubules seems to counteract strain-induced mechanical stress levels. Such lateral microtubule reinforcement has been described already for compressive loads.[54] Our data suggest that this may also account for strained neuronal extensions.[17] In addition, reinforcement does not seem to be exclusively dependent on MAP2 since an increase in MAP2 protein levels was lower compared to gained microtubule levels. It is therefore conceivable that straining triggers other proteins to replace MAP2. Since MAP2 is a well-established neuronal differentiation marker [55] one would naturally expect a MAP2 replacement by other microtubule binding proteins upon neuronal maturation with axon and dendrite formation.[56]

Summary and Conclusion

The vital importance of mechanical cues in neuronal development is a matter of current debate. To date, little is known about the response of primary neurons to mechanical stimuli. We investigated the response of primary cortical neurons to cyclic strain with physiologically relevant amplitudes and repeat frequencies.[23-24] Despite a drastic immediate response to strain that was indicated by a retraction of neurite branches, formation of retraction bulbs, and a collapsed microtubule network, neurons were able to adapt to cyclic stretch conditions without any sign of apoptosis. Furthermore, cyclic stretching over hours induces outgrowth in low strain direction with overall enhanced growth rates and enhanced neuronal branch formation. On the molecular level, we observed that the mechanical stress response depends on the angle relative to stretch and goes along with clear adaptations in microtubule and MAP2 protein content. Taken together, our study demonstrates that while neurons display strong reactions to mechanical strain, they are well able to survive and adapt to such mechanical stress conditions. We could therefore highlight a vital role of mechanical stimuli and suggest that strain as occurs, for example, due to brain function related diameter changes of blood vessels [24] might be an important key modulator and trigger of certain processes in neuronal development.

Supporting Information

Typical results of the image processing algorithms, movie showing cellular reactions to cyclic stretch.

References

1. Barnes, J. M.; Przybyla, L., Tissue mechanics regulate brain development, homeostasis and disease. **2017,** *130* (1), 71-82.
2. Smith, D. H., Stretch growth of integrated axon tracts: Extremes and exploitations. *Progress in neurobiology* **2009,** *89* (3), 231-239.
3. Lu, Y.-B.; Franze, K.; Seifert, G.; Steinhäuser, C.; Kirchhoff, F.; Wolburg, H.; Guck, J.; Janmey, P.; Wei, E.-Q.; Käs, J.; Reichenbach, A., Viscoelastic properties of individual glial cells and neurons in the CNS. *Proceedings of the National Academy of Sciences of the United States of America* **2006,** *103* (47), 17759-17764.
4. LaPlaca, M.; Prado, G. R., Neural Mechanobiology and Neuronal Vulnerability to Traumatic Loading. *J Biomech* **2010,** *43*, 71-78.
5. Fletcher, D. A.; Mullins, R. D., Cell mechanics and the cytoskeleton. *Nature* **2010,** *463* (7280), 485-92.
6. Janmey, P. A.; Euteneuer, U.; Traub, P.; Schliwa, M., Viscoelastic properties of vimentin compared with other filamentous biopolymer networks. *J Cell Biol* **1991,** *113* (1), 155-60.
7. Tang-Schomer, M. D.; Patel, A. R.; Baas, P. W.; Smith, D. H., Mechanical breaking of microtubules in axons during dynamic stretch injury underlies delayed elasticity, microtubule disassembly, and axon degeneration. *Faseb j* **2010,** *24* (5), 1401-10.
8. Kevenaar, J. T.; Hoogenraad, C. C., The axonal cytoskeleton: from organization to function. *Frontiers in Molecular Neuroscience* **2015,** *8*, 44.
9. Dehmelt, L.; Halpain, S., The MAP2/Tau family of microtubule-associated proteins. *Genome Biol* **2005,** *6* (1), 204.
10. Subramanian, R.; Kapoor, Tarun M., Building Complexity: Insights into Self-Organized Assembly of Microtubule-Based Architectures. *Developmental Cell* **2012,** *23* (5), 874-885.
11. Rosenberg, K. J.; Ross, J. L.; Feinstein, H. E.; Feinstein, S. C.; Israelachvili, J., Complementary dimerization of microtubule-associated tau protein: Implications for microtubule bundling and tau-mediated pathogenesis. *Proc Natl Acad Sci U S A* **2008,** *105* (21), 7445-50.
12. Peter, S. J.; Mofrad, M. R. K., Computational Modeling of Axonal Microtubule Bundles under Tension. *Biophysical Journal* **2012,** *102* (4), 749-757.
13. Higgins, S.; Lee, J. S.; Ha, L.; Lim, J. Y., Inducing neurite outgrowth by mechanical cell stretch. *Biores Open Access* **2013,** *2* (3), 212-6.
14. Koser, D. E.; Thompson, A. J.; Foster, S. K.; Dwivedy, A.; Pillai, E. K.; Sheridan, G. K.; Svoboda, H.; Viana, M.; Costa, L. D.; Guck, J.; Holt, C. E.; Franze, K., Mechanosensing is critical for axon growth in the developing brain. *Nat Neurosci* **2016,** *19* (12), 1592-1598.
15. Pfister, B. J.; Iwata, A.; Meaney, D. F.; Smith, D. H., Extreme Stretch Growth of Integrated Axons. *The Journal of Neuroscience* **2004,** *24* (36), 7978-7983.
16. Pfister, B. J.; Bonislawski, D. P.; Smith, D. H.; Cohen, A. S., Stretch-grown axons retain the ability to transmit active electrical signals. *FEBS Lett* **2006,** *580* (14), 3525-31.
17. Lamoureux, P.; Heidemann Steven, R.; Martzke Nathan, R.; Miller Kyle, E., Growth and elongation within and along the axon. *Developmental Neurobiology* **2009,** *70* (3), 135-149.

18. Loverde, J. R.; Tolentino, R. E.; Pfister, B. J., Axon Stretch Growth: The Mechanotransduction of Neuronal Growth. *Journal of Visualized Experiments : JoVE* **2011,** (54), 2753.
19. Nguyen, T. D.; Hogue, I. B.; Cung, K.; Purohit, P. K.; McAlpine, M. C., Tension-induced neurite growth in microfluidic channels. *Lab Chip* **2013,** *13* (18), 3735-40.
20. Bayly, P. V.; Cohen, T. S.; Leister, E. P.; Ajo, D.; Leuthardt, E.; Genin, G. M., Deformation of the human brain induced by mild acceleration. *Journal of neurotrauma* **2005,** *22* (8), 845-856.
21. Fleming, S.; Thompson, M.; Stevens, R.; Heneghan, C.; Pluddemann, A.; Maconochie, I.; Tarassenko, L.; Mant, D., Normal ranges of heart rate and respiratory rate in children from birth to 18 years of age: a systematic review of observational studies. *Lancet* **2011,** *377* (9770), 1011-8.
22. Wedeen, V. J.; Ponceleti, B., Brain Parenchyma Motion Observed by MRI. In *eMagRes*.
23. Drew, P. J.; Shih, A. Y.; Kleinfeld, D., Fluctuation and Sensory-Induced Vasodynamics in Rodent Cortex Extend Arteriole Capacity. *Proc Natl Acad Sci USA* **2011,** *108*, 8473-8478.
24. Mateo, C.; Knutsen, P. M.; Tsai, P. S.; Shih, A. Y.; Kleinfeld, D., Entrainment of Arteriole Vasomotor Fluctuations by Neural Activity is a Basis of Blood-Oxygenation-Level-Dependent "Resting-State" Connectivity. *Neuron* **2017,** *96*, 936-948.
25. Martin, G. T., Acute brain trauma. *Annals of The Royal College of Surgeons of England* **2016,** *98* (1), 6-10.
26. El Sayed, T.; Mota, A.; Fraternali, F.; Ortiz, M., Biomechanics of traumatic brain injury. *Computer Methods in Applied Mechanics and Engineering* **2008,** *197* (51), 4692-4701.
27. Niediek, V.; Born, S.; Hampe, N.; Kirchgessner, N.; Merkel, R.; Hoffmann, B., Cyclic stretch induces reorientation of cells in a Src family kinase- and p130Cas-dependent manner. *Eur J Cell Biol* **2012,** *91* (2), 118-28.
28. Berthier, E.; Young, E. W. K.; Beebe, D., Engineers are from PDMS-Land, Biologists are from Polystyrenia. *Lab on a Chip* **2012,** *12*, 1224-1237.
29. Morris, E. J.; Geller, H. M., Induction of neuronal apoptosis by camptothecin, an inhibitor of DNA topoisomerase-I: evidence for cell cycle-independent toxicity. *J Cell Biol* **1996,** *134* (3), 757-70.
30. Hersch, N.; Wolters, B.; Dreissen, G.; Springer, R.; Kirchgessner, N.; Merkel, R.; Hoffmann, B., The constant beat: cardiomyocytes adapt their forces by equal contraction upon environmental stiffening. *Biol Open* **2013,** *2* (3), 351-61.
31. Rueden, C. T.; Schindelin, J.; Hiner, M. C.; DeZonia, B. E.; Walter, A. E.; Arena, E. T.; Eliceiri, K. W., ImageJ2: ImageJ for the next generation of scientific image data. *BMC Bioinformatics* **2017,** *18* (1), 529.
32. Li, W.; Tang, Q. Y.; Jadhav, A. D.; Narang, A.; Qian, W. X.; Shi, P.; Pang, S. W., Large-scale topographical screen for investigation of physical neural-guidance cues. *Sci Rep* **2015,** *5*, 8644.
33. Tondon, A.; Hsu, H.-J.; Kaunas, R., Dependence of cyclic stretch-induced stress fiber reorientation on stretch waveform. *Journal of Biomechanics* **2012,** *45* (5), 728-735.
34. Sawada, Y.; Tamada, M.; Dubin-Thaler, B. J.; Cherniavskaya, O.; Sakai, R.; Tanaka, S.; Sheetz, M. P., Force sensing by mechanical extension of the Src family kinase substrate p130Cas. *Cell* **2006,** *127* (5), 1015-26.
35. Faust, U.; Hampe, N.; Rubner, W.; Kirchgeßner, N.; Safran, S.; Hoffmann, B.; Merkel, R., Cyclic Stress at mHz Frequencies Aligns Fibroblasts in Direction of Zero Strain. *PLOS ONE* **2011,** *6* (12), e28963.

36. Shaohui Cui, S. Z., Huiying Chen, Bing Wang, Yinan Zhao, Defu Zhi The Mechanism of Lipofectamine 2000 Mediated Transmembrane Gene Delivery *Engineering* **2012,** *5*, 172-75.
37. Haq, F.; Keith, C.; Zhang, G., Neurite development in PC12 cells on flexible micro-textured substrates under cyclic stretch. *Biotechnol Prog* **2006,** *22* (1), 133-40.
38. Morrison, B., 3rd; Cater, H. L.; Wang, C. C.; Thomas, F. C.; Hung, C. T.; Ateshian, G. A.; Sundstrom, L. E., A tissue level tolerance criterion for living brain developed with an in vitro model of traumatic mechanical loading. *Stapp Car Crash J* **2003,** *47*, 93-105.
39. Hayakawa, K.; Hosokawa, A.; Yabusaki, K.; Obinata, T., Orientation of Smooth Muscle-Derived A10 Cells in Culture by Cyclic Stretching: Relationship between Stress Fiber Rearrangement and Cell Reorientation. *Zoological science* **2000,** *17* (5), 617-24.
40. Hayakawa, K.; Sato, N.; Obinata, T., Dynamic reorientation of cultured cells and stress fibers under mechanical stress from periodic stretching. *Exp Cell Res* **2001,** *268* (1), 104-14.
41. Wang, J. H.; Goldschmidt-Clermont, P.; Wille, J.; Yin, F. C., Specificity of endothelial cell reorientation in response to cyclic mechanical stretching. *J Biomech* **2001,** *34* (12), 1563-72.
42. Jungbauer, S.; Gao, H.; Spatz, J. P.; Kemkemer, R., Two characteristic regimes in frequency-dependent dynamic reorientation of fibroblasts on cyclically stretched substrates. *Biophys J* **2008,** *95* (7), 3470-8.
43. Dent, E. W.; Kalil, K., Axon Branching Requires Interactions between Dynamic Microtubules and Actin Filaments. *The Journal of Neuroscience* **2001,** *21* (24), 9757.
44. Fukushima, N., *Microtubules in the Nervous System*. 2011; Vol. 3, p 55-71.
45. Kalil, K.; Dent, E. W., Branch management: mechanisms of axon branching in the developing vertebrate CNS. *Nat Rev Neurosci* **2014,** *15* (1), 7-18.
46. Flynn, K. C.; Hellal, F.; Neukirchen, D.; Jacob, S.; Tahirovic, S.; Dupraz, S.; Stern, S.; Garvalov, B. K.; Gurniak, C.; Shaw, A. E.; Meyn, L.; Wedlich-Soldner, R.; Bamburg, J. R.; Small, J. V.; Witke, W.; Bradke, F., ADF/cofilin-mediated actin retrograde flow directs neurite formation in the developing brain. *Neuron* **2012,** *76* (6), 1091-107.
47. Kapitein, L. C.; Hoogenraad, C. C., Building the Neuronal Microtubule Cytoskeleton. *Neuron* **2015,** *87* (3), 492-506.
48. Yokota, Y.; Kim, W. Y.; Chen, Y.; Wang, X.; Stanco, A.; Komuro, Y.; Snider, W.; Anton, E. S., The adenomatous polyposis coli protein is an essential regulator of radial glial polarity and construction of the cerebral cortex. *Neuron* **2009,** *61* (1), 42-56.
49. Pacheco, A.; Gallo, G., Actin Filament-Microtubule Interactions in Axon Initiation and Branching. *Brain Res Bull* **2016,** *126*, 300-310.
50. Hawkins, T.; Mirigian, M.; Selcuk Yasar, M.; Ross, J. L., Mechanics of microtubules. *J Biomech* **2010,** *43* (1), 23-30.
51. Mitchison, T.; Kirschner, M., Dynamic instability of microtubule growth. *Nature* **1984,** *312* (5991), 237-42.
52. Geiger, R. C.; Kaufman, C. D.; Lam, A. P.; Budinger, G. R.; Dean, D. A., Tubulin acetylation and histone deacetylase 6 activity in the lung under cyclic load. *Am J Respir Cell Mol Biol* **2009,** *40* (1), 76-82.
53. Schaedel, L.; John, K.; Gaillard, J.; Nachury, M. V.; Blanchoin, L.; Thery, M., Microtubules self-repair in response to mechanical stress. *Nat Mater* **2015,** *14* (11), 1156-63.
54. Brangwynne, C. P.; MacKintosh, F. C.; Kumar, S.; Geisse, N. A.; Talbot, J.; Mahadevan, L.; Parker, K. K.; Ingber, D. E.; Weitz, D. A., Microtubules can bear enhanced compressive

loads in living cells because of lateral reinforcement. *The Journal of Cell Biology* **2006,** *173* (5), 733-741.
55. Soltani, M. H.; Pichardo, R.; Song, Z.; Sangha, N.; Camacho, F.; Satyamoorthy, K.; Sangueza, O. P.; Setaluri, V., Microtubule-associated protein 2, a marker of neuronal differentiation, induces mitotic defects, inhibits growth of melanoma cells, and predicts metastatic potential of cutaneous melanoma. *Am J Pathol* **2005,** *166* (6), 1841-50.
56. Dehmelt, L.; Halpain, S., The MAP2/Tau family of microtubule-associated proteins. *Genome biology* **2005,** *6* (1), 204-204.

Figure legends

Figure 1. Neuronal viability after strain. (**A** and **B**) Cortical neurons without and with cyclic strain at indicated parameters. DIC live cell imaging after 24 h of cyclic straining (**A**) and immunocytochemical staining against MAP2 and tubulin (**B**) after 6 days of stretch are indicated. Direction of uniaxial cyclic strain is indicated by the black arrow. (**C**) Cells were stained with ethidium homodimer to investigate the number of dead cells after 24 h of cyclic stretch and subsequently analyzed by flow cytometry. Camptothecin was used as positive control for induced cell death. Note the unchanged cell viability even at highest strain amplitudes. Scale bars = 100 µm.

Figure 2. Directional neurite outgrowth of stretched neurons. (**A**) Cortical neurons were stretched for 24 h with indicated amplitudes, fixed, and subsequently stained for tubulin and MAP2. Cells without straining were used as control. Direction of uniaxial cyclic strain is indicated by the black arrow and holds for all micrographs. (**B**) For all cells, main branch orientation was determined and is given as cumulative frequency. For each condition the analysis includes at least six independent experiments with always more than 550 analyzed cells. Reorientation intensity was amplitude dependent and the highest for 28%. All images were equally contrast and brightness enhanced. Scale bar = 100 µm.

Figure 3. Increased neurite growth and branching in response to strain. (**A**) Cortical neurons were stretched for 24 h with indicated amplitudes and stained for MAP2 and tubulin. Primary extensions (white arrowhead) and side branches (white arrow) are indicated. (**B**) Using image processing routines overall number of side branches as well as (**C**) summed-up length of all branches per cell were determined. Results in (**B**) and (**C**) are

depicted as mean ± 95% confidence intervals: control 27.3 ± 1.5; 7% 33. 4 ± 1.2; 15% 30.9 ± 1.4, 28% 30.6 ± 1.7 branches per cell (B); control 113.9 ± 5.9 μm; 7% 145 ± 5.3 μm; 15% 133.5 ± 5.9 μm; 28% 131.6 ± 6.9 μm (**C**). For all parameters the analysis included at least 6 independent experiments per parameter with always more than 550 cells analyzed for each condition. Black double arrow depicts direction of uniaxial cyclic strain and applies to all micrographs. Scale bar = 20 μm.

Figure 4. Spontaneous response to cyclic stretch. (**A** and **B**) Neurons were grown for 6 days on elastomeric substrates to allow for network formation and then stretched with an amplitude of 15% and a frequency of 300 mHz. (**A**) Neurons were observed for 30 min before stretch (left) during cyclic stretch for 1 h (middle), and after cyclic stretch for 30 min (right) by DIC live cell microscopy. Analyzed cell extensions were specifically chosen for their orientation relative to stretch (perpendicular (top), diagonal (middle), and parallel (bottom)). Strain induced formation of retraction bulbs is highlighted by yellow arrows. The black arrow indicates the direction of strain and applies to all micrographs. (**B**) Microtubules were stained with Tubulin Tracker™ Green and analyzed by live cell microscopy upon strain application. Note the strain-induced loss of microtubules behind the growth cone and high concentrations of destabilized and curled microtubule structures in formed retraction bulbs. Scale bar in (**A**) = 25 μm; scale bar in (**B**) = 5 μm**.**

Figure 5. Angle dependent cytoskeletal protein localization in cyclically stretched cells. Neurons stretched for 24 h with indicated amplitudes were stained for MAP2 and tubulin. Subsequently image processing routines separated neuronal extensions branches (for details see Experimental section). Intensities for MAP2 (**A**) and tubulin (**B**) are plotted as mean (bars denote standard error of mean) in an angle dependent manner. The analysis included at least 4 independent experiments for each strain condition, with always more than 400 cells analyzed for each condition and over 200 data point for each angle and condition indicated.

Supplementary Figure 1. Data processing of immunofluorescence images. Quantitative analysis of the immunofluorescence image (**A**) was performed by an in house developed software. Using various processing routines as described in the experimental section, neurons were identified based on immunofluorescent images stained for tubulin and MAP2.

Neurons were stretched for 24 h with an amplitude of 28% and a frequency of 300 mHz. The uniaxial stretch direction in this image is vertical, while cells grew perpendicular in the horizontal direction. Exemplarily, one neuron is indicated (white box) and further analyzed in (**B**). Here, a mask was generated and skeletonized to detect nodal (green crosses) and end points (yellow crosses) of the neurites for each individual neuron. An ellipse was fitted around each detected neurite branch to analyze the branch orientation. The branch orientations of detected ellipses for all cells detected in (**A**) are depicted in **C**. Scale bar = 100 µm.

Supplementary Movie 1. Spontaneous response to cyclic stretch. Neurons were grown for 6 days and then stretched with an amplitude of 15% and a frequency of 300 mHz while simultaneously recorded via DIC live cell microscopy. Neurons were observed 30 min prior stretch, 60 min during stretch and 30 min after cyclic stretch. Images recorded within the period of cyclic stretch are highlighted with a red arrow that is additionally indicating the direction of stretch. Analyzed cell extensions were specifically chosen for their orientation relative to stretch (**A**: perpendicular, **B:** diagonal and **C:** parallel). Scale bar = 25 µm.

Figure 1

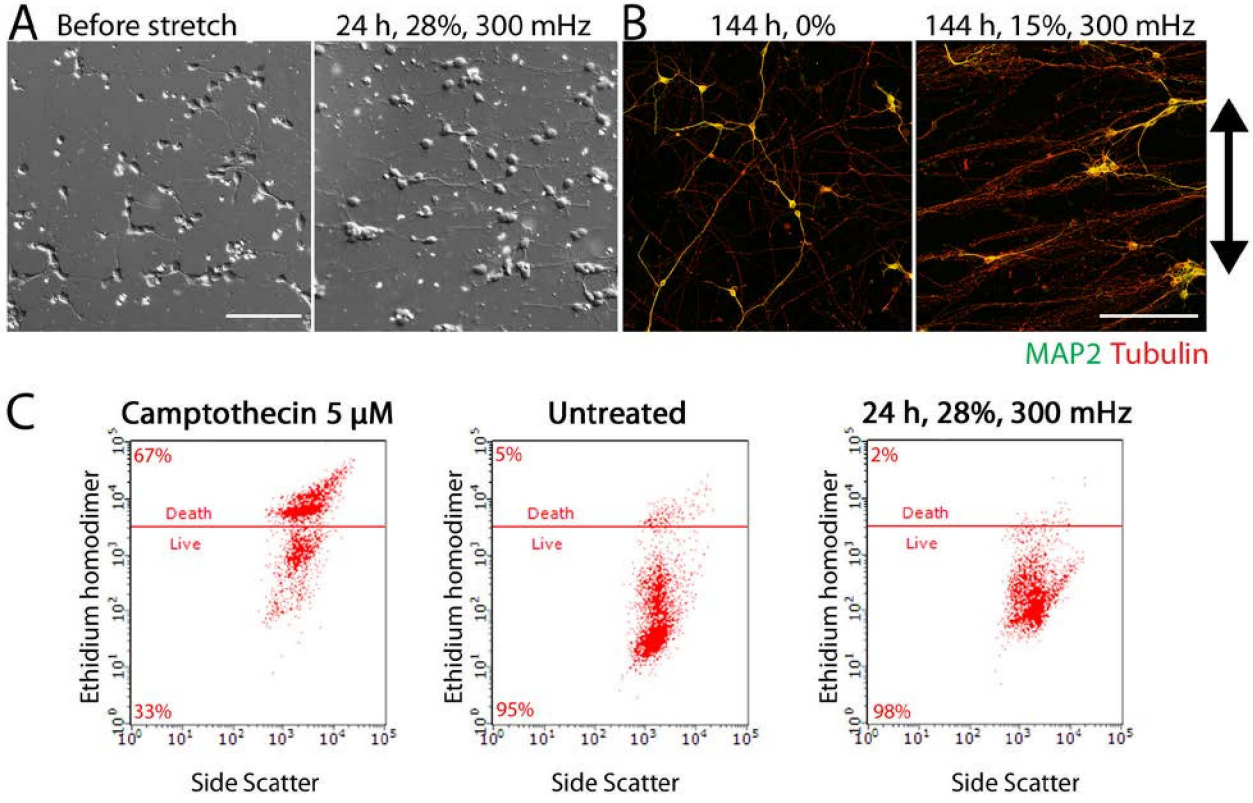
A
Before stretch
24 h, 28%, 300 mHz
B
144 h, 0%
144 h, 15%, 300 mHz
MAP2 Tubulin
C
Camptothecin 5 µM
Untreated
24 h, 28%, 300 mHz
Ethidium homodimer
Side Scatter
67%
33%
5%
95%
2%
98%
Death
Live

Figure 2

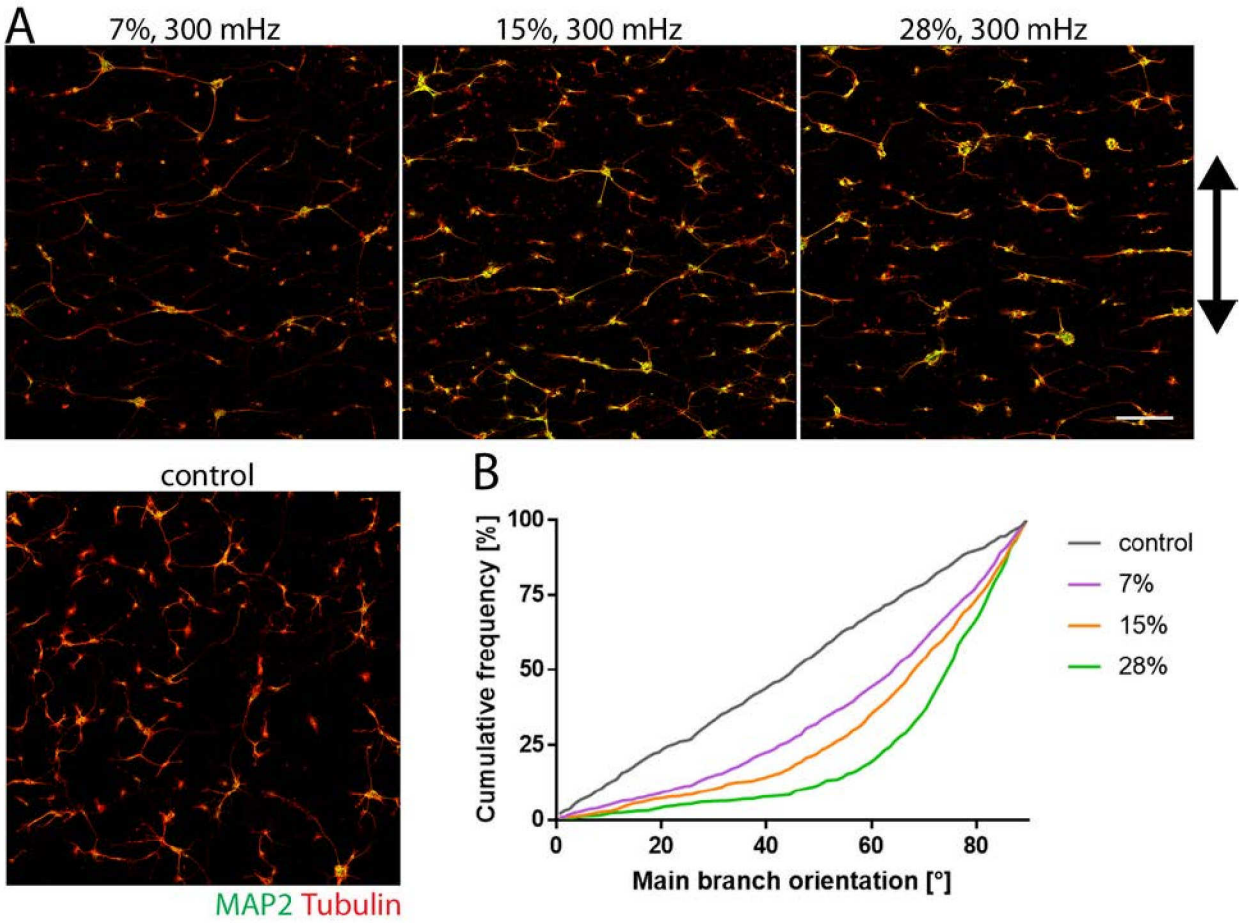
A
7%, 300 mHz
15%, 300 mHz
28%, 300 mHz
control
MAP2 Tubulin
B
Cumulative frequency [%]
100
75
50
25
0
0
20
40
60
80
Main branch orientation [°]
control
7%
15%
28%

Figure 3

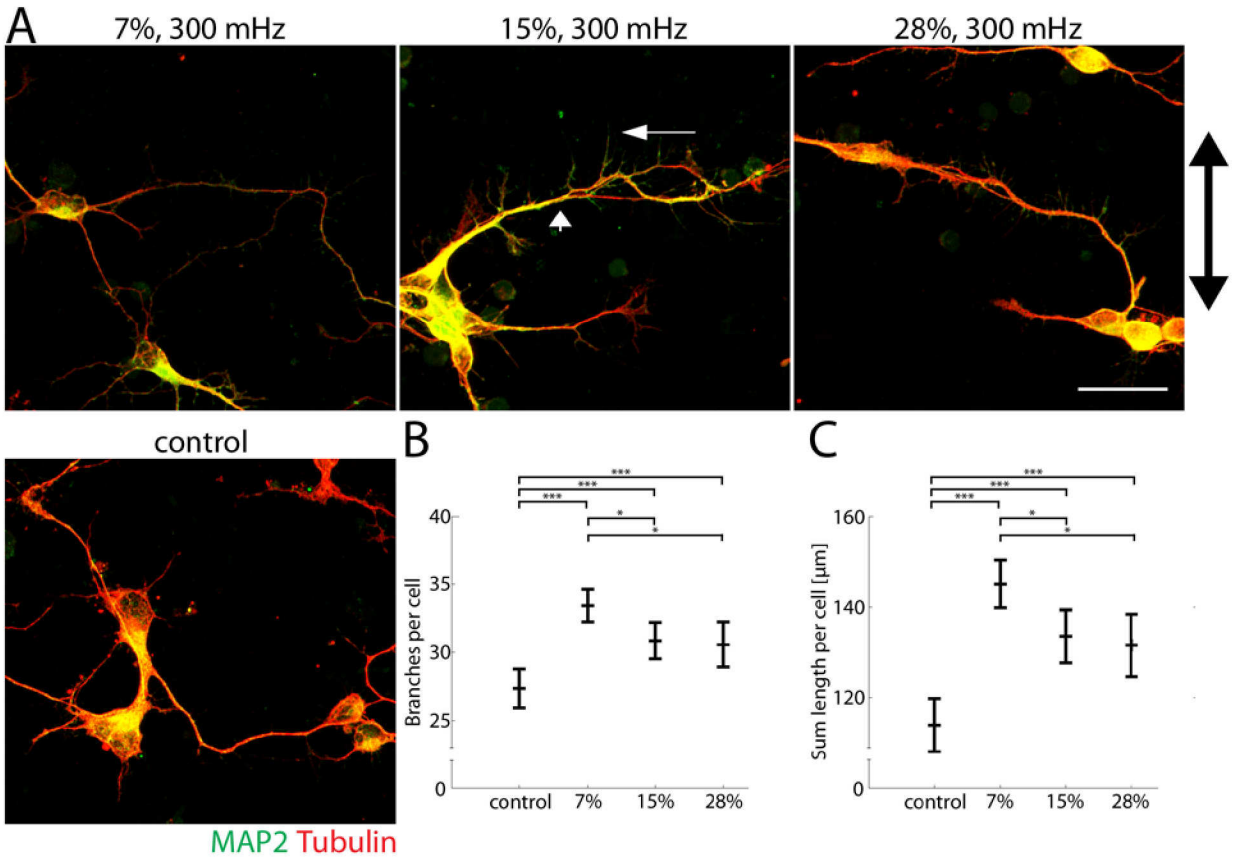
A
7%, 300 mHz
15%, 300 mHz
28%, 300 mHz
control
MAP2 Tubulin
B
Branches per cell
40
35
30
25
0
control
7%
15%
28%
***
***
***
*
*
C
Sum length per cell [µm]
160
140
120
0
control
7%
15%
28%
***
***
***
*
*

Figure 4

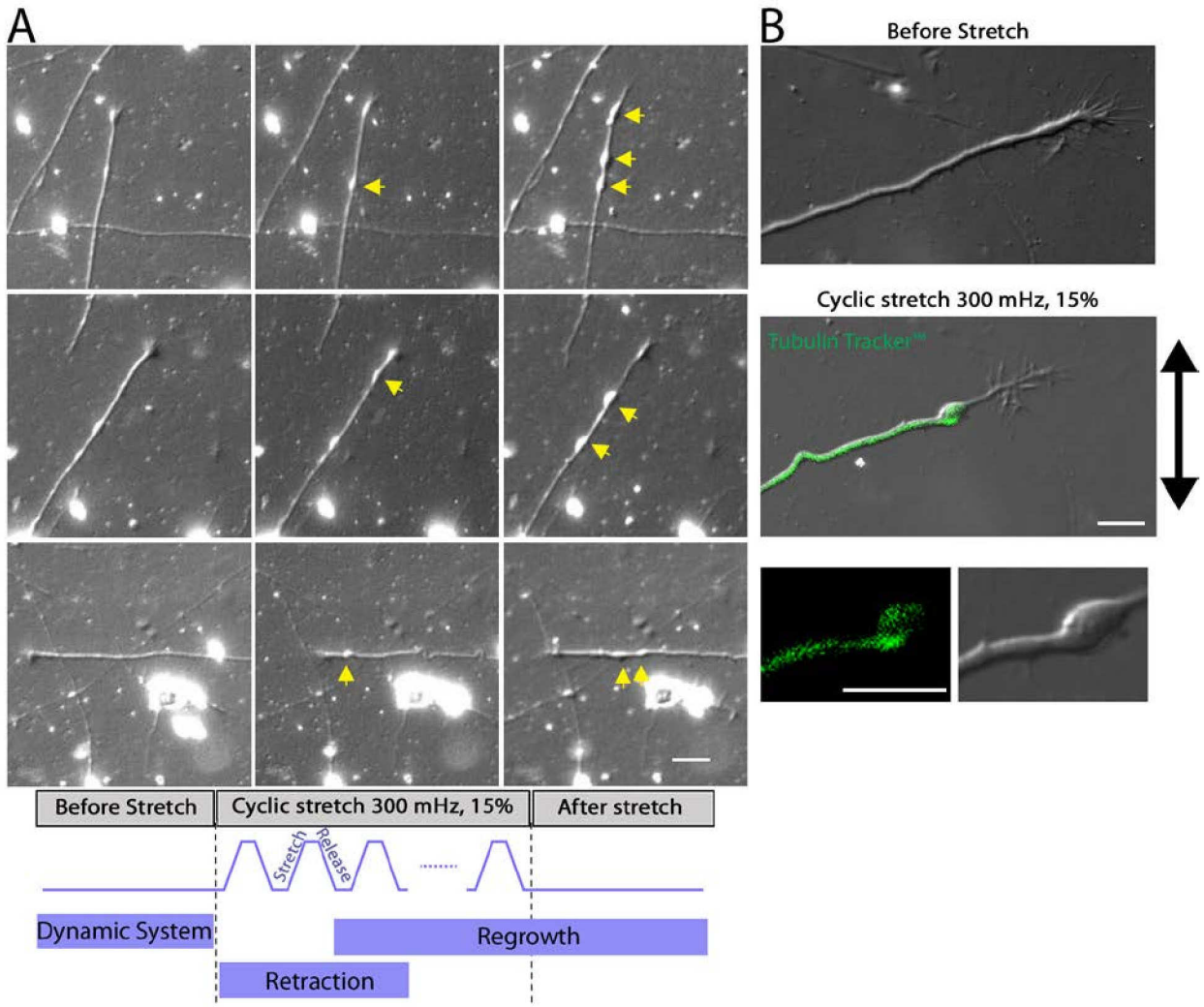
A
B
Before Stretch
Cyclic stretch 300 mHz, 15%
Tubulin Tracker™
Before Stretch
Cyclic stretch 300 mHz, 15%
After stretch
Stretch
Release
Dynamic System
Regrowth
Retraction

Figure 5

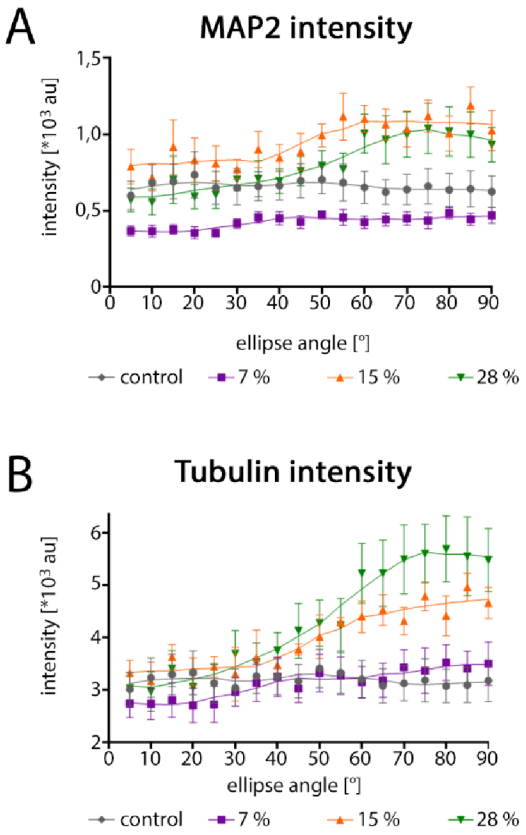
A
MAP2 intensity
intensity [*10³ au]
1,5
1,0
0,5
0
0 10 20 30 40 50 60 70 80 90
ellipse angle [°]
control
7 %
15 %
28 %
B
Tubulin intensity
intensity [*10³ au]
6
5
4
3
2
0 10 20 30 40 50 60 70 80 90
ellipse angle [°]
control
7 %
15 %
28 %

Supplementary Figure 1

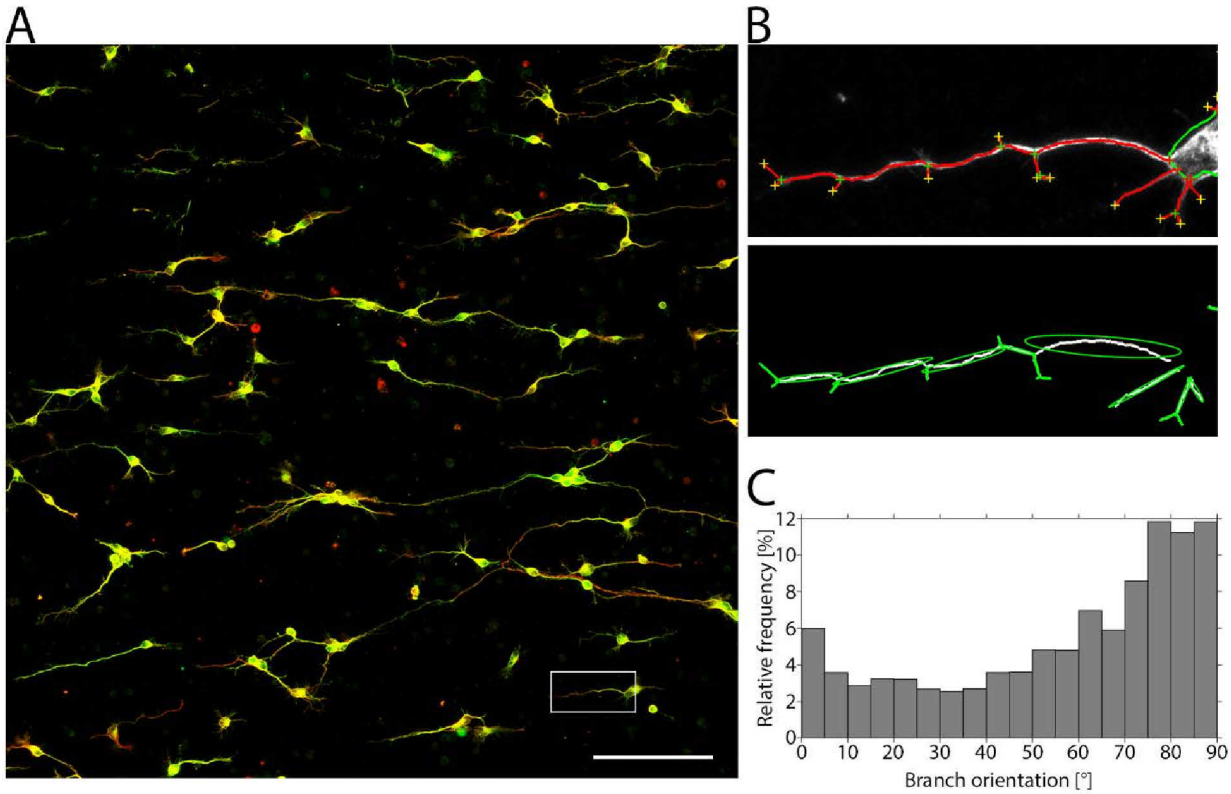

For Table of Contents Only